with the trans-Pt–S distance ~0.05 Å longer than the cis-Pt–S distances. Since data to only $\theta \cong 22.5°$ were collected and disorder may exist in the ethoxy groups, further detailed discussion of the structural features appears unwarranted.

The structure of $[Pd(S_2PPh_2)(PEt_3)_2]S_2PPh_2$ is unambiguously that of a four-coordinate (PdS_2P_2) cation with a dithiolate anion. The Pd–S distances are equal to within two standard deviations (Table IX) for the bonded atoms and comparable to the trans-Pd–S distance in $Pd(S_2PPh_2)_2PPh_3$. Distances and angles generally are comparable in the two structures for similarly bonded atoms. The anionic ligand shows a S–P–S angle of 117.9 (8)°, only slightly larger than the 113.9 (10)° angle of the dangling ligand in $Pd(S_2PPh_2)_2PPh_3$.

In addition to evidence for each of the structures observed in the solid state for phosphine adducts of 1,1-dithiolate, phosphine exchange also occurs in solution. The ^{31}P NMR line shape observed for $Pd(S_2P(OEt)_2)_2PPh_3$ above −20 °C clearly shows this by loss of P–P coupling. Over the same temperature range this phosphine exchange is much slower with the Pt than with the analogous Pd complexes.

The activation energy $\Delta G^{\ddagger}$ of 12.4 kcal/mol at −27 °C is comparable with the ^1H results (12.5 kcal/mol) reported previously[3a] for uni-/bidentate $^-S_2P(OEt)_2$ ligand exchange in $Pt(S_2P(OEt)_2)_2PPh_3$. The fact that the apparent T_1 for both dithiophosphate P atoms is the same (and shorter than the lifetime for exchange) suggests that the equivalence is due to the exchange process and hence likely an intramolecular process. Intramolecular exchange has been established[2a] to be the process producing equivalent ligands in $Pt(Se_2CN(i\text{-}Bu)_2)_2PR_3$. A full line-shape analysis of the ^1H NMR spectra of various $Pt(S–S)_2L$ complexes is also consistent with this conclusion.[3b]

The ^{13}C NMR spectra of $Pt(S_2CN(i\text{-}Bu)_2)_2PMe_2Ph$ in $CDCl_3$ (with added CH_2Cl_2 at −70 °C show resonances to be expected from the geometry found in the solid. The dangling dithiolate ligand cis to the phosphine shows no $^{31}P–^{13}C$ coupling while the bidentate ligand displays a $^2J_{C-Pt}$ of 56 Hz. With Pt compounds cis couplings are generally near zero and always much smaller than trans coupling constants.[19]

The result of this work on phosphine adducts of nickel triad 1,1-dithiolates is summarized in Scheme I. Each species now has been identified crystallographically. Exchange rates generally are faster with Pd than with Pt analogues at a given temperature. No five- or six-coordinate species have been isolated with Pd^{II} or Pt^{II} as the metal ions, although a five-coordinate species can be obtained[20] with Ni^{II}. Dynamic NMR data implicate[2a] the formation of five-coordinate species as intermediates with Pd and Pt.

Acknowledgment. The support of NSF Grant CHE-8013141 for structural studies and Grant NIH GM-19050 for dynamical measurements is acknowledged for the work performed at CWRU. The studies at EU benefited from generous loans of K_2PtCl_4 and $PdCl_2$ from Johnson Matthey Ltd. Matthey Bishop, Inc., supplied a generous quantity of $PdCl_2$ for the work at CWRU. The support (to J.M.C.A. and A.J.F.F.) from the SRC also is acknowledged. Crystallographic calculations at EU made use of the "X-ray 72" computer programs. The effort of David Briggs to check tables is greatly appreciated.

Registry No. $Pt(S_2CNEt_2)_2PPh_3$, 40545-16-2; $Pd(S_2PPh_2)_2PPh_3$, 29894-52-8; $Pt(S_2P(OEt)_2)_2PPh_3$, 40537-11-9; $[Pd(S_2PPh_2)(PEt_3)_2]S_2PPh_2$, 29894-48-2.

Supplementary Material Available: Tables S-I to S-VIII, listing thermal parameters and structure factors (20 pages). Ordering information is given on any current masthead page.

Contribution from the Department of Chemistry, University of Auckland, Private Bag, Auckland, New Zealand

Spectroelectrochemistry of Nickel Complexes. Voltammetric and ESR Studies of the Redox Reactions of Phosphine–Dithiolate and Phosphine–Catecholate Complexes of Nickel

G. A. BOWMAKER,* P. D. W. BOYD, and G. K. CAMPBELL

Received October 27, 1981

The redox properties of nickel(II) complexes of the type $[Ni(PPh_3)_2L]^{n+}$ (L = dithiolate (n = 0) or dithiocarbamate (n = 1)) and Ni(dpe)L (dpe = bis(diphenylphosphino)ethane, L = dithiolate or catecholate) have been studied by cyclic voltammetry at a platinum electrode, and the products of the redox reactions have been identified by electron spin resonance spectroscopy. All of these complexes show reversible or quasi-reversible one-electron reduction processes, and the reduction potentials for the PPh_3 complexes are about 0.5 V higher than those of the corresponding dpe complexes. In the case of triphenylphosphine complexes such as $Ni(PPh_3)_2((CN)_2C_2S_2)$, the voltammetry shows evidence of a dissociation equilibrium involving loss of triphenylphosphine from the nickel species present after the electron-transfer process. The frozen-solution ESR spectra of the reduction products show large, anisotropic hyperfine coupling to two equivalent ^{31}P nuclei and anisotropic g values characteristic of d^9 nickel(I) species. The PPh_3 complexes have smaller ^{31}P hyperfine coupling constants than the corresponding dpe complexes. The ^{31}P hyperfine coupling parameters have been analyzed for some representative complexes, and the amount of spin density transferred from the metal to the phosphine ligands has been estimated. In addition to the reduction process, the catecholate complexes undergo a reversible one-electron oxidation. The ESR spectra of the products of such oxidations show only a small ^{31}P hyperfine coupling, hyperfine coupling to nuclei in the catecholate ligand, and almost isotropic g values. These species are therefore formulated as nickel(II) complexes containing coordinated semiquinone radical anions.

Introduction

Transition-metal dithiolene complexes have been the subject of a considerable amount of research over the past 20 years, and several reviews dealing with the unusual chemical and physical properties of these complexes have been published.[1–5] One of the most interesting properties of these compounds is their ability to undergo facile electron-transfer reactions, and

(1) McCleverty, J. A. *Prog. Inorg. Chem.* **1968**, *10*, 49.
(2) Schrauzer, G. N. *Acc. Chem. Res.* **1969**, *2*, 72.

0020-1669/82/1321-2403$01.25/0

the structural and spectroscopic changes which accompany these reactions have attracted much attention.

We have recently shown that the cationic complexes $[Ni(dpe)(R_2NCS_2)]^+$ (R = ethyl, butyl, benzyl, cyclohexyl; dpe = bis(diphenylphosphino)ethane, $Ph_2PCH_2CH_2PPh_2$) can be reduced electrochemically in a quasi-reversible one-electron step to form neutral nickel(I) complexes $Ni(dpe)(R_2NCS_2)$, which can be detected by ESR spectroscopy, and which subsequently undergo a disproportionation to give the nickel(0) and nickel(II) complexes $Ni(dpe)_2$ and $Ni(R_2NCS_2)_2$.[6]

The previously reported nickel(II) complex $Ni(PPh_3)_2((CN)_2C_2S_2)$ is closely related to these dithiocarbamate complexes, but it has been stated that this complex does not readily undergo redox reactions.[7] We have carried out a more detailed investigation of the redox chemistry of this and the corresponding dithiocarbamate complexes $[Ni(PPh_3)_2(S_2CNR_2)]^+$ using cyclic voltammetry and have identified one-electron reduction products by means of ESR spectroscopy. Similar electrochemical and ESR studies have also been carried out on $Ni(dpe)((CN)_2C_2S_2)$ and several other nickel(II) complexes containing one bidentate phosphine or arsine ligand (bis(diphenylphosphino)methane (dpm), bis(diphenylphosphino)ethane (dpe), bis(diphenylphosphino)butane (dpb), bis(diphenylarsino)ethane (dae)) and one of the following dithiolate or catecholate ligands: **1** = maleonitriledithiolate, $(CN)_2C_2S_2^{2-}$; **2** = toluenedithiolate, $CH_3C_6H_3S_2^{2-}$; **3** = dithiooxalate, $O_2C_2S_2^{2-}$; **4** = trithiocarbonate, CS_3^{2-}; **5** = *o*-xylenedithiolate, $C_6H_4(CH_2S)_2^{2-}$; **6** = catecholate, $C_6H_4O_2^{2-}$; **7** = tetrachlorocatecholate, $C_6Cl_4O_2^{2-}$. Of the dithiolates listed, only maleonitriledithiolate is known to stabilize a nickel(I) complex: $[Ni((CN)_2C_2S_2)_2]^{3-}$.[8-10] As a general rule maleonitriledithiolate tends to stabilize the more reduced forms while toluenedithiolate stabilizes the more oxidized forms of transition-metal complexes.[1,11,12] Catecholate ligands form transition-metal complexes which undergo electrochemical or chemical oxidations which are believed to involve oxidation of the catecholate ligand rather than the metal.[13-19] However, no reductions of nickel(II) complexes of these ligands have been reported to date. We have found that the mixed-ligand phosphine–catecholate complexes undergo one-electron reduction processes similar to those observed for the corresponding dithiolate complexes. The catecholate complexes were found to undergo quasi-reversible one-electron oxidation processes as well, and these reactions were studied by means of cyclic voltammetry and ESR spectroscopy.

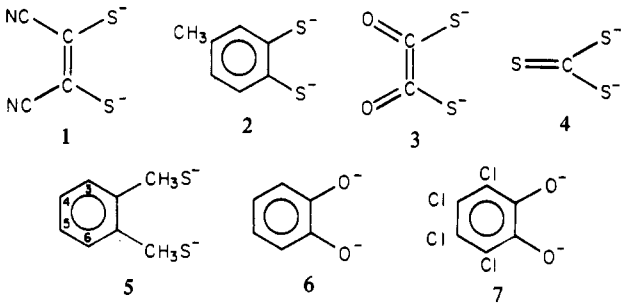

Experimental Section

$Ni(PPh_3)_2((CN)_2C_2S_2)$[7] and $[Ni(PPh_3)_2(R_2NCS_2)]PF_6$[20] were prepared by literature methods.

Preparation of Ni(dpm)((CN)$_2$C$_2$S$_2$). A solution of dpm (0.39 g, 1 mmol) in acetone (25 mL) was added to $Ni(PPh_3)_2((CN)_2C_2S_2)$ (0.72 g, 1 mmol) in acetone (25 mL). The solution was stirred for 1 h. The bulk of the acetone was then removed by suction and upon the slow addition of hexane afforded precipitation of the complex. The light brown solid was filtered, washed with diethyl ether, and recrystallized from dichloromethane/*o*-xylene; mp 278–80 °C. Anal. Calcd for $C_{29}H_{22}N_2NiP_2S_2$: C, 59.72; H, 3.80; N, 4.80. Found: C, 59.38; H, 4.38; N, 4.83.

Preparation of Ni(dae)((CN)$_2$C$_2$S$_2$). A solution of dae (0.49 g, 1 mmol) in acetone (25 mL) was added to $Ni(PPh_3)_2((CN)_2C_2S_2)$ (0.72 g, 1 mmol) in acetone (25 mL). The solution was stirred until no more solid remained. The bulk of the acetone was removed by suction, and hexane was then added to afford precipitation. The brown solid was filtered from solution, washed with ether, and recrystallized from dichloromethane/*o*-xylene; mp 270 °C. Anal. Calcd for $C_{30}H_{24}As_2N_2NiS_2$: C, 52.58; H, 3.53; N, 4.09. Found: C, 52.58; H, 3.63; N, 4.11.

Preparation of Ni(dpe)((CN)$_2$C$_2$S$_2$). $Na_2((CN)_2C_2S_2)$ (0.19 g, 1 mmol) and $Ni(dpe)Cl_2$ (0.53 g, 1 mmol) were mixed as solids, and acetone (40 mL) was added. The resulting solution was stirred for 30 min and then filtered (to remove NaCl). The complex was precipitated by the slow addition of water, with vigorous stirring. The orange solid was filtered from the solution, washed with diethyl ether, and then recrystallized from dichloromethane/diethyl ether; mp >330 °C. Anal. Calcd for $C_{30}H_{24}N_2NiP_2S_2$: C, 60.32; H, 4.05; N, 4.69. Found: C, 60.37; H, 4.15; N, 4.50.

Preparation of Ni(dpe)(O$_2$C$_2$S$_2$). $K_2(O_2C_2S_2)$ (0.17 g, 1 mmol) and $Ni(dpe)Cl_2$ (0.53 g, 1 mmol) were added to dichloromethane (50 mL) under a N_2 atmosphere. The solution was stirred for 30 min and then filtered and the volume reduced to approximately 10 mL by suction. Upon the slow addition of hexane an orange solid separated. The solid was filtered from solution and recrystallized from dichloromethane/diethyl ether; mp 296 °C. Anal. Calcd for $C_{28}H_{24}O_2NiP_2S_2$: C, 58.26; H, 4.16; P, 10.73. Found: C, 58.26; H, 4.64; P, 10.62.

Preparation of Ni(dpe)(CS$_3$). K_2CS_3 (0.19 g, 1 mmol) and $Ni(dpe)Cl_2$ (0.53 g, 1 mmol) in an acetone/water (30/5) mixture was stirred for 1 h under a N_2 atmosphere. The solution was filtered, and further water was slowly added to afford precipitation of the complex. The orange solid was filtered from the solution, washed with diethyl ether, and then recrystallized from dichloromethane/diethyl ether; mp 218–219 °C. Anal. Calcd for $C_{27}H_{24}NiP_2S_3$: C, 57.37; H, 4.28. Found: C, 57.08; H, 4.36.

Preparation of Ni(dpe)(CH$_3$C$_6$H$_3$S$_2$). To a slurry of $Ni(dpe)Cl_2$ (0.68 g, 1.27 mmol) in a solution of toluenedithiol (0.20 g, 1.27 mmol) in methanol (30 mL), under a nitrogen atmosphere, was added a NaOMe/MeOH solution (2.5 mL, 1.0 mol L^{-1}; 2.5 mmol). The solution was stirred for 3 h, and then water was slowly added to afford further precipitation of the complex. The solution was filtered and the pink solid washed with diethyl ether and then recrystallized from dichloromethane/diethyl ether; mp 292 °C. Anal. Calcd for $C_{33}H_{30}NiP_2S_2$: C, 64.83; H, 4.95. Found: C, 64.96; H, 4.79.

(3) Eisenberg, R. *Prog. Inorg. Chem.* **1970**, *12*, 295.
(4) Hoyer, E. *Z. Chem.* **1971**, *11*, 41.
(5) Burns, R. P.; McAuliffe, C. A. *Adv. Inorg. Chem. Radiochem.* **1979**, *22*, 303.
(6) Bowmaker, G. A.; Boyd, P. D. W.; Campbell, G. K.; Hope, J. M.; Martin, R. L. *Inorg. Chem.* **1982**, *21*, 1152.
(7) Davidson, A.; Edelstein, N.; Holm, R. H.; Maki, A. H. *Inorg. Chem.* **1964**, *3*, 814.
(8) Mines, T. E.; Geiger, W. E., Jr. *Inorg. Chem.* **1973**, *12*, 1189.
(9) Geiger, W. E., Jr.; Mines, T. E.; Senftleber, F. C. *Inorg. Chem.* **1975**, *14*, 2141.
(10) Geiger, W. E., Jr.; Allen, C. S.; Mines, T. E.; Senftleber, F. C. *Inorg. Chem.* **1977**, *16*, 2003.
(11) McCormick, B. J.; Rinehart, D. S. *J. Inorg. Nucl. Chem.* **1980**, *42*, 928.
(12) Williams, R.; Billig, E.; Waters, J. H.; Gray, H. B. *J. Am. Chem. Soc.* **1966**, *88*, 43.
(13) Rohrscheid, F.; Balch, A. L.; Holm, R. H. *Inorg. Chem.* **1966**, *5*, 1542.
(14) Balch, A. L. *J. Am. Chem. Soc.* **1973**, *95*, 2723.
(15) Razuvaev, G. A.; Teplova, I. A.; Shalnova, K. G.; Abakumov, G. A. *J. Organomet. Chem.* **1978**, *353*, 157.
(16) Abakumov, G. A.; Teplova, I. A.; Cherkasov, V. K.; Shalnova, K. G. *Inorg. Chim. Acta* **1979**, *32*, L57.
(17) Wilshire, J. P.; Leon, L.; Bosserman, P.; Sawyer, D. T. *J. Am. Chem. Soc.* **1979**, *101*, 3379.
(18) Wicklund, P. A.; Beckman, L. S.; Brown, D. G. *Inorg. Chem.* **1976**, *15*, 1996.
(19) Brown, D. G.; Hemphill, W. D. *Inorg. Chem.* **1979**, *18*, 2039.
(20) McCleverty, J. A.; Morrison, N. J. *J. Chem. Soc., Dalton Trans.* **1976**, *541*.

Preparation of Ni(dpe)($C_6H_4(CH_2S)_2$). To a slurry of $Ni(dpe)Cl_2$ (0.53 g, 1.0 mmol) in a solution of *o*-xylenedithiol (0.17 g, 1.0 mmol), in methanol (20 mL) under a N_2 atmosphere, was added NaOMe/MeOH (2.0 mL, 1 mol L^{-1}; 2 mmol). The solution was stirred for 30 min, and then water (50 mL) was added to effect precipitation of the product. The solution was further stirred for 1 h and then filtered. The green solid was washed with MeOH and hexane and then dried in vacuo; mp 226 °C. Anal. Calcd for $C_{34}H_{32}NiP_2S_2$: C, 65.24; H, 5.16. Found: C, 64.30; H, 5.40.

Preparation of Ni(dpe)($C_6H_4O_2$). To a slurry of $Ni(dpe)Cl_2$ (0.53 g, 1 mmol) in a methanol (30 mL) solution of catechol (0.11 g, 1 mmol) under a N_2 atmosphere was added NaOMe/MeOH (2.0 mL, 1 mol L^{-1}; 2 mmol). The color of the solution changed from orange to dark green in a 5-min time period. The solution was stirred for a further 30 min, water (50 mL) was slowly added, and the solution was stirred for a further 30 min. The green solid was then filtered, washed with water and ether, and then recrystallized from CH_2Cl_2/ether and dried in vacuo; mp 250–251 °C. Anal. Calcd for $C_{32}H_{28}NiO_2P_2$: C, 68.00; H, 4.99. Found: C, 67.77; H, 4.96.

The corresponding 4-methylcatecholate and 4-*tert*-butylcatecholate compounds $Ni(dpe)(CH_3C_6H_3O_2)$ and $Ni(dpe)(t\text{-}BuC_6H_3O_2)$ were prepared in a similar manner with the appropriate catechols. $Ni(dpe)(CH_3C_6H_3O_2)$ is a green solid; mp 239 °C. Anal. Calcd for $C_{33}H_{30}NiO_2P_2$: C, 68.43; H, 5.22. Found: C, 68.13; H, 5.50. The *tert*-butylcatecholate complex was obtained as a dichloromethane solvate, $Ni(dpe)(t\text{-}BuC_6H_3O_2)\cdot 0.5CH_2Cl_2$, and is a green solid; mp 217 °C. Anal. Calcd for $C_{36.5}H_{37}ClNiO_2P_2$: C, 66.04; H, 5.62. Found: C, 65.74; H, 6.10.

Preparation of Ni(dpe)($C_6Cl_4O_2$). To a slurry of $Ni(dpe)Cl_2$ (0.53 g, 1 mmol) in a methanol (30 mL) solution of tetrachlorocatechol (0.25 g, 1 mmol), under a N_2 atmosphere, was added NaOMe/MeOH (2.0 mL, 1 mol L^{-1}; 2 mmol). The color of the solution changed from orange to brown. The solution was stirred for 1 h, and then water (50 mL) was slowly added. The brown solid was then filtered from solution and washed with water, methanol, and hexane. The solid was recrystallized from CH_2Cl_2/*o*-xylene and dried in vacuo; mp 255 °C. Anal. Calcd for $C_{32}H_{24}Cl_4NiO_2P_2$: C, 54.67; H, 3.44. Found: C, 54.27; H, 3.97.

Preparation of Ni(dpb)($(CN)_2C_2S_2$). $Na_2((CN)_2C_2S_2)$ (0.19 g, 1 mmol), $NiCl_2\cdot 6H_2O$ (0.23 g, 1 mmol), and dpb (0.42 g, 1 mmol) were mixed as solids, and acetone (40 mL) was added. The resulting solution was stirred for 3 h and then filtered (to remove NaCl). The complex was precipitated by the slow addition of water, with vigorous stirring. The brown solid was filtered from the solution, washed with diethyl ether, and then recrystallized from dichloromethane/ethanol; mp 271 °C. Anal. Calcd for $C_{32}H_{28}N_2NiP_2S_2$: C, 61.46; H, 4.51. Found: C, 60.96; H, 4.90.

Electrochemistry. Electrochemical measurements were carried out at a platinum electrode (surface area 0.28 cm^2) with a PAR 173 potentiostat with PAR 179 digital coulometer with IR compensation, ECG 175 universal programmer, and HP 7046A X-Y recorder. The reference electrode was Ag/AgCl (0.1 M LiCl in CH_2Cl_2) separated from the voltammetric cell by a 0.1 M $(Bu_4N)ClO_4$ in CH_2Cl_2 salt bridge. Measurements were carried out in dichloromethane (0.1 M $(Bu_4N)ClO_4$ supporting electrolyte) or in acetonitrile (0.1 M $(Bu_4N)ClO_4$ supporting electrolyte). All potentials were internally referenced to the potential for the one-electron oxidation of ferrocene (+0.46 V vs. Ag/AgCl) or the one-electron oxidation of $[Pt((CN)_2C_2S_2)_2]^{2-}$ (+0.16 V vs. Ag/AgCl) as described previously.[6]

Electron Spin Resonance Spectra. X-Band electron spin resonance spectra were recorded with a Varian E4 spectrometer. The electrochemically produced species were generated in situ on a platinum electrode by controlled-potential electrolysis using a three-electrode configuration,[6] at potentials slightly beyond the measured redox potential of the complex. Electrolyses in this cell could be carried out at ambient or lower temperatures with the Varian variable-temperature attachment. Frozen-solution spectra were obtained by freezing the contents of the in situ cell after electrolysis.

The method used to simulate frozen-solution spectra has been described previously.[6]

Results and Discussion

Preparation and Properties of the Nickel(II) Complexes. The compounds $Ni(PPh_3)_2((CN)_2C_2S_2)$[7] and $[Ni(PPh_3)_2(R_2NCS_2)]PF_6$[20] have been described by other workers. In the present work mixed-ligand complexes containing bidentate phosphines and dithiolate or catecholate ligands were prepared either from the corresponding bis(triphenylphosphine) complex by displacement of the PPh_3 by the bidentate phosphine (eq 1) or from the $NiCl_2$ complex of the bidentate phosphine by

$$Ni(PPh_3)_2((CN)_2C_2S_2) + dpm \rightarrow Ni(dpm)((CN)_2C_2S_2) + 2PPh_3 \quad (1)$$

displacement of Cl^- by the dithiolate or catecholate ligand (eq 2).

$$Ni(dpe)Cl_2 + (CN)_2C_2S_2^{2-} \rightarrow Ni(dpe)((CN)_2C_2S_2) + 2Cl^- \quad (2)$$

The compound $Ni(diphos)(C_6Cl_4O_2)$, which was prepared in the present work from tetrachlorocatecholate by the second of the above methods, has been reported previously as the product of an oxidative addition reaction of tetrachloro-*o*-benzoquinone, $C_6Cl_4O_2$, with the zerovalent compound $Ni(dpe)(CO)_2$[21] (eq 3).

$$Ni(dpe)(CO)_2 + C_6Cl_4O_2 \rightarrow Ni(dpe)(C_6Cl_4O_2) + 2CO \quad (3)$$

All of the nickel(II) complexes prepared are diamagnetic and so probably have cis square-planar structures. They are air stable in the solid state. The tetrachlorocatecholate and catecholate complexes are not very air stable in solution.

The ^{13}C and ^{31}P NMR spectra of the triphenylphosphine complexes were examined in order to obtain information about the stability of these complexes with respect to loss of PPh_3. Due to its higher solubility, the best results were obtained for $[Ni(PPh_3)_2(Bu_2NCS_2)]PF_6$.

The ^1H noise-decoupled ^{13}C spectrum of this compound in $CDCl_3$ is as follows (δ (multiplicity)): 13.5 (s), 19.6 (s), 29.1 (s), 49.2 (s), 127.6 (quintet), 128.7 (t), 131.5 (s), 134.0 (t), 198.5 (t). The singlets in the range 10–50 ppm are assigned to the butyl carbons, and the triplet at 198.5 ppm is assigned to the dithiocarbamate carbon. The splitting of this signal is due to coupling with the two equivalent ^{31}P (J = 4.9 Hz). The signals in the range 127–134 ppm are assigned to the phenyl carbons of the coordinated PPh_3 (cf. 129–139 ppm in uncomplexed PPh_3[22]). Some of these signals display multiplet structure which is due to coupling of the carbon nuclei to the ^{31}P nucleus in the same PPh_3 molecule and to virtual coupling to the ^{31}P nucleus in the other PPh_3 molecule in the complex. Virtual coupling of this type is due to strong ^{31}P–^{31}P coupling and is often observed in complexes where the phosphine molecules in the complex are trans to each other. It is also known to occur, however, in some complexes where the phosphines are mutually cis, as in the present case.[23] There were no signals in the spectrum which could be attributed to free PPh_3. Hence, if a dissociation involving loss of PPh_3 is occurring, the exchange between free and complexed PPh_3 would have to be sufficiently fast to give an exchange-averaged spectrum. However, if this were the case, the spectrum would not be expected to show the effects of ^{31}P coupling to nuclei external to the PPh_3 molecule in which it is situated (such coupling would be averaged to zero by the exchange). Since these effects are observed (^{31}P–^{13}C coupling to the dithiocarbamate carbon and strong ^{31}P–^{31}P coupling), it appears that processes involving rapid exchange of the PPh_3 molecules do not occur in solutions of this complex. However, addition of

(21) Barlex, D. M.; Kemmitt, R. D. W.; Littlecott, G. W. *J. Organomet. Chem.* **1972**, *43*, 225.
(22) Bundgaard, T.; Jakobsen, H. J. *Acta Chem. Scand.* **1972**, *26*, 2548. Braterman, P. S.; Milne, D. W.; Randall, E. W.; Rosenberg, E. *J. Chem. Soc., Dalton Trans.* **1973**, 1027.
(23) Pregosin, P. S.; Kunz, R. W. In "N.M.R. Basic Principles and Progress"; Diehl, P., Fluck, E., Kosfeld, R., Eds.; Springer-Verlag: Berlin, 1979; Vol. 15, p 65.

Table I. Cyclic Voltammetry Parameters for One-Electron Reduction and Oxidation Reactions of Some Nickel(II) Complexes in Dichloromethane at ca. 290 K[a]

compd	redn			oxidn		
	$E_{1/2}$, V	ΔE_{pp},[d] V	ΔE_{pp},[e] V	$E_{1/2}$, V	ΔE_{pp},[d] V	ΔE_{pp},[e] V
$[Ni(PPh_3)_2(Et_2NCS_2)]^+$	−0.70	0.14	0.20			
$[Ni(PPh_3)_2(Bu_2NCS_2)]^+$	−0.71	0.20	0.22			
$[Ni(PPh_3)_2(Bzl_2NCS_2)]^+$	−0.65	0.20	0.24			
$[Ni(PPh_3)_2(Cy_2NCS_2)]^+$	−0.78	0.19	0.23			
$Ni(PPh_3)_2((CN)_2C_2S_2)$	−0.74	0.07	0.09			
$Ni(dpe)((CN)_2C_2S_2)$	−1.20	0.06	0.07			
$Ni(dpm)((CN)_2C_2S_2)$	−1.08	0.06	0.06			
$Ni(dpb)((CN)_2C_2S_2)$	−1.06	0.20	0.22			
$Ni(dae)((CN)_2C_2S_2)$	−0.98	0.09	0.10			
$Ni(dpe)(CH_3C_6H_3S_2)$	−1.59	0.13	0.20			
$Ni(dpe)(C_6H_4(CH_2S)_2)$	−1.50	0.16	0.17			
$Ni(dpe)(O_2C_2S_2)$	−1.19	0.09	0.10			
$Ni(dpe)(CS_3)$	−1.41	0.06	0.07			
$Ni(dpe)(C_6Cl_4O_2)$	−1.24	0.10	0.12	+0.71	0.06	0.07
$Ni(dpe)(C_6H_4O_2)$	−1.44	0.12	0.13	+0.31	0.09	0.10
$Ni(dpe)(CH_3C_6H_3O_2)$	−1.50	0.12	0.13	+0.22	0.08	0.11
$Ni(dpe)(t\text{-}BuC_6H_3O_2)$	−1.51	0.10	0.13	+0.21	0.09	0.10
$[Ni((CN)_2C_2S_2)_2]^{2-}$	−1.70	0.20	0.25			
$Ni(Bu_2NCS_2)_2$	−1.62[b]					
$[Ni(dpe)_2]^{2+}$	−0.23[c]					

[a] For the ferrocene/ferrocenium couple at 0.46 V relative to Ag/AgCl 0.1 M LiCl. [b] Measured by a.c. cyclic voltammetry. [c] Reference 6. [d] At 100 mV s^{-1}. [e] At 200 mV s^{-1}.

Table II. ESR Parameters for Nickel(I) Complexes Electrogenerated in Dichloromethane, Isotropic Parameters from Solution Spectra at −40 °C, and Anisotropic Parameters from Frozen-Solution Spectra at −160 °C (Parameters Defined in Figure 8)

complex	g	g_1	g_2	g_3	a^a	$A_1{}^a$	$A_2{}^a$	$A_3{}^a$
$Ni(PPh_3)_2(Et_2NCS_2)$	2.138	2.251	2.067	*b*	*c*	55.2	63.7	*b*
$Ni(PPh_3)_2(Bu_2NCS_2)$	2.135	2.245	2.062	*b*	*c*	55	62	*b*
$Ni(PPh_3)_2(Bzl_2NCS_2)$	2.141	2.258	2.064	*b*	*c*	58.0	60.0	*b*
$Ni(PPh_3)_2(Cy_2NCS_2)$	2.129	2.241	2.063	*b*	*c*	56.8	63.8	*b*
$[Ni(PPh_3)_2((CN)_2C_2S_2)]^-$	2.082	2.214	2.066	*b*	90.9	87.9	95.2	*b*
$[Ni(dpe)((CN)_2C_2S_2)]^-$	2.079	2.161	2.043	2.036	103.7	92.3	102.5	112.2
$[Ni(dpm)((CN)_2C_2S_2)]^-$	2.081	2.187	2.049	*b*	97.1	104.7	98.0	*b*
$[Ni(dpb)((CN)_2C_2S_2)]^-$	2.094	2.177	2.045	2.045	98.5	92.7	102.6	102.6
$[Ni(dae)((CN)_2C_2S_2)]^-$	2.105	2.226	2.058	*b*	110.4	103.9	115.3	*b*
$[Ni(dpe)(CH_3C_6H_3S_2)]^-$	2.062	2.172	2.053	2.033	102.3	90.8	98.2	111.5
$[Ni(dpe)(O_2C_2S_2)]^-$	2.091	2.187	2.047	2.038	90.8	81.7	83.6	97.5
$[Ni(dpe)(CS_3)]^-$	2.080	2.186	2.054	2.045	88.7	79.1	79.1	93.1
$[Ni(dpe)(C_6Cl_4O_2)]^-$	2.077	2.188	2.055	2.034	93.9	91.9	95.0	106.8
$[Ni(dpe)(C_6H_4O_2)]^-$	2.080	2.179	2.058	2.035	91.0	78.8	85.0	96.0

[a] Coupling constants given in 10^{-4} cm^{-1}. [b] Spectra are axially symmetric ($g_2 = g_3$, $A_2 = A_3$). [c] ^{31}P hyperfine structure not resolved in solution spectra.

excess PPh_3 causes loss of the ^{31}P–^{13}C virtual coupling and the ^{31}P–^{13}C coupling to the dithiocarbamate carbon, so it appears that significant exchange of the PPh_3 ligand occurs under these conditions.

The ^{31}P NMR spectrum of $[Ni(PPh_3)_2Bu_2NCS_2]PF_6$ consists of a single line (175.8 ppm) due to the PPh_3 phosphorus nuclei and a septet due to the PF_6 (used as reference, 0 ppm). Addition of further PPh_3 to the solution resulted in the appearance of a new signal, assigned to uncoordinated PPh_3, at 138.8 ppm. Further additions of PPh_3 amounting to more than a tenfold excess relative to the nickel complex resulted in an increase in intensity of the uncoordinated PPh_3 signal and a slight broadening of the complexed PPh_3 signal but no shift in the line positions. These results indicate that the nickel complex does not dissociate to give free PPh_3 in solution and that added PPh_3 does not coordinate to the complex or undergo rapid exchange with the coordinated PPh_3 molecules.

Reduction of $Ni^{II}(dpe)((CN)_2C_2S_2)$ and Related Complexes. $Ni^{II}(dpe)((CN)_2C_2S_2)$ showed a reversible reduction in CH_2Cl_2 solvent (Figure 1), and the cyclic voltammetry parameters are given in Table I. Controlled-potential electrolysis in the in situ ESR cell resulted in spectra (Figure 2) showing hyperfine coupling to two equivalent ^{31}P nuclei and anisotropic g values (Table II) similar in magnitude to those observed earlier for the $[Ni^I(dpe)(R_2NCS_2)]$ complexes.[6] Thus, the ESR spectra

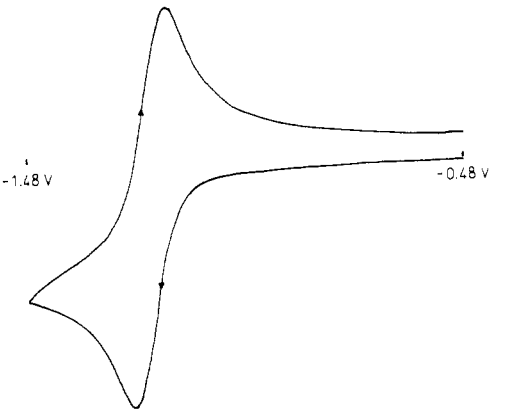

Figure 1. Cyclic voltammogram of $Ni^{II}(dpe)((CN)_2C_2S_2)$ in CH_2Cl_2 (scan rate = 100 mV s^{-1}).

are attributed to a Ni^I complex produced by a one-electron reduction of the parent Ni^{II} complex:

$$Ni^{II}(dpe)((CN)_2C_2S_2) + e^- \rightarrow [Ni^I(dpe)((CN)_2C_2S_2)]^- \quad (4)$$

A series of related complexes in which bis(diphenylphosphino)ethane was replaced by the bidentate phosphine or

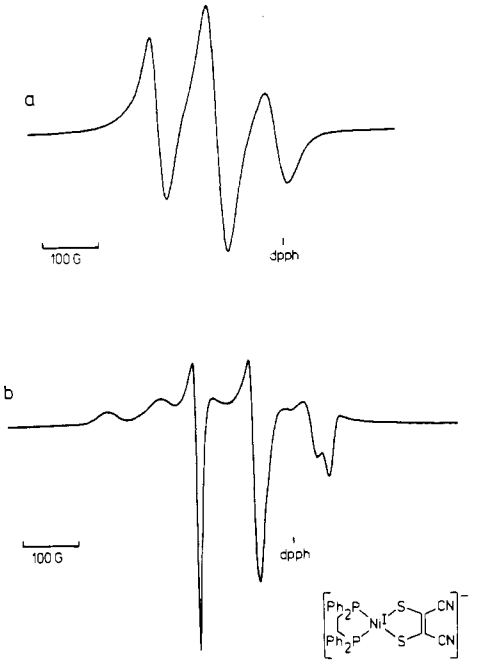

Figure 2. ESR spectra of $[Ni^{I}(dpe)((CN)_2C_2S_2)]^-$ electrogenerated in CH_2Cl_2 at −40 °C: (a) solution spectrum at −40 °C; (b) frozen-solution spectrum at −160 °C.

arsine ligands (bis(diphenylphosphino)methane (dpm), bis(diphenylphosphino)butane (dpb), bis(diphenylarsino)ethane (dae)) and maleonitriledithiolate was replaced by the bidentate dithiolate ligands toluenedithiolate, dithiooxalate, trithiocarbonate, and *o*-xylenedithiolate (see Introduction) were studied in a similar manner. Reversible or quasi-reversible reductions were observed in each case, and the cyclic voltammetry parameters are given in Table I. For all but the $Ni^{II}(dpe)(C_6H_4(CH_2S)_2)$ complex, the products were identified by their ESR spectra, which showed hyperfine coupling to two equivalent P or As atoms and coupling constants and *g* values (Table II) similar in magnitude to those of $[Ni^{I}(dpe)((CN)_2C_2S_2)]^-$. In the case of $Ni^{II}(dpe)(C_6H_4(CH_2S)_2)$, the cyclic voltammogram showed a large separation between the anodic and cathodic peaks, and this separation increased markedly with increasing sweep rate. This suggests that electron transfer is the rate-limiting step in the electrode process involved. The reduction product in this case was not sufficiently stable to allow an ESR spectrum to be obtained.

None of the above compounds showed reversible oxidation reactions. Oxidation processes were observed in the voltammograms in the range 0–1 V in some cases, but these were generally complex and irreversible.

Reduction of $[Ni^{II}(PPh_3)_2(R_2NCS_2)]^+$ and $Ni^{II}(PPh_3)_2((CN)_2C_2S_2)$. All of these compounds were found to undergo a single reduction process in the range 0 to −2 V. The reductions are irreversible in the absence of added PPh_3. On addition of excess triphenylphosphine to the solutions prior to examination by cyclic voltammetry, the ratio of the anodic to cathodic peak heights increases and approaches unity at high concentrations of added phosphine. This indicates that the reductions approach complete chemical reversibility as the concentration of added PPh_3 is increased. Typical cyclic voltammograms for the reduction of $Ni(PPh_3)_2((CN)_2C_2S_2)$ for a series of concentrations of added phosphine are shown in Figure 3. Cyclic voltammetry parameters for the above reductions in the presence of excess PPh_3 are listed in Table I.

Electrolysis of the solutions (with excess PPh_3 present) at the appropriate potential in the in situ ESR cell produced species which gave strong ESR signals. In the case of $[Ni(PPh_3)_2(R_2NCS_2)]^+$, the resulting spectra were very broad (width at half-height σ = 250 G) and showed no resolved ^{31}P hyperfine structure. This can be contrasted with the spectra observed on reduction of the corresponding bis(diphenylphosphino)ethane compounds $[Ni(dpe)(R_2NCS_2)]^+$, which showed narrower lines and hyperfine coupling to two equivalent ^{31}P nuclei.[6] The solution spectrum obtained on reduction of $Ni(PPh_3)_2((CN)_2C_2S_2)$ showed narrower lines, however, and the expected hyperfine coupling to two equivalent ^{31}P nuclei was resolved (Figure 4). The hyperfine coupling constant is given in Table II. In all cases the frozen-solution spectra showed well-resolved ^{31}P hyperfine structure (Figures 4 and 5) and anisotropic *g* values (Table II) similar in magnitude to those observed earlier for the $[Ni(dpe)(R_2NCS_2)]^+$ complexes.[6] Thus, by analogy with this previous work, the ESR spectra are attributed to Ni^{I} complexes produced by a one-electron reduction of the parent Ni^{II} complex (eq 5).

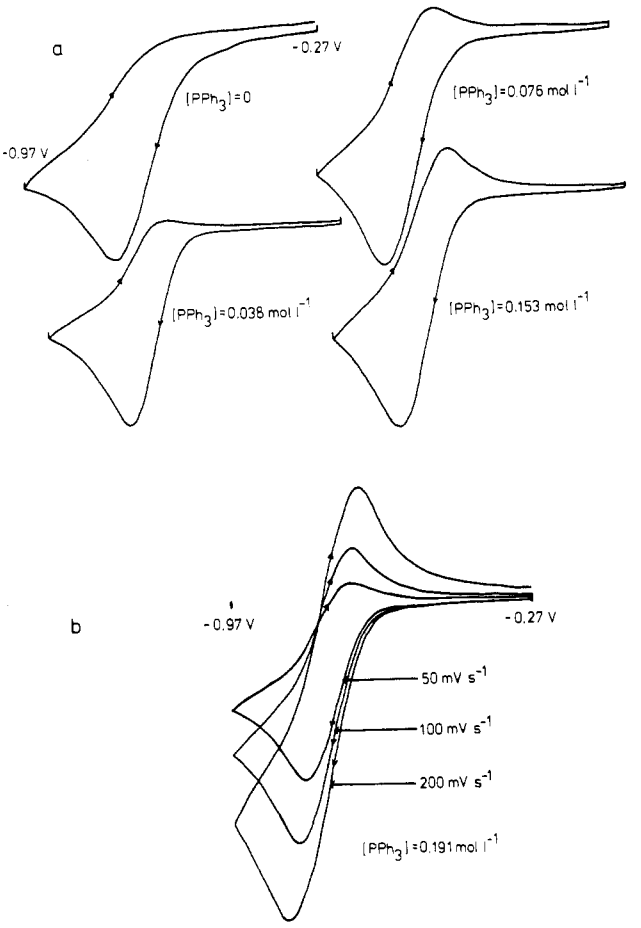

Figure 3. Cyclic voltammograms of $Ni^{II}(PPh_3)_2((CN)_2C_2S_2)$ in CH_2Cl_2 for various concentrations of added triphenylphosphine ($[Ni(PPh_3)_2((CN)_2C_2S_2)]$ = 0.07 mol L^{-1}): (a) scan rate = 100 mV s^{-1}; (b) scan rates as shown.

$$[Ni^{II}(PPh_3)_2(R_2NCS_2)]^+ + e^- \rightarrow Ni^{I}(PPh_3)_2(R_2NCS_2) \quad (5)$$

The cyclic voltammograms for the one-electron reduction of $Ni^{II}(PPh_3)_2((CN)_2C_2S_2)$ show a scan rate dependence typical of an EC process, i.e., an electrochemical reduction followed by a chemical reaction of the reduction product $[Ni^{I}(PPh_3)_2((CN)_2C_2S_2)]^-$ (Figure 3). ESR measurements show that the decay of this species follows first-order kinetics, and analysis of the cyclic voltammograms according to the method of Nicholson and Shain for a first-order EC process[24] shows that the apparent rate constant k' is proportional to the

(24) Nicholson, R. S.; Shain, I. *Anal. Chem.* **1964**, *36*, 706.

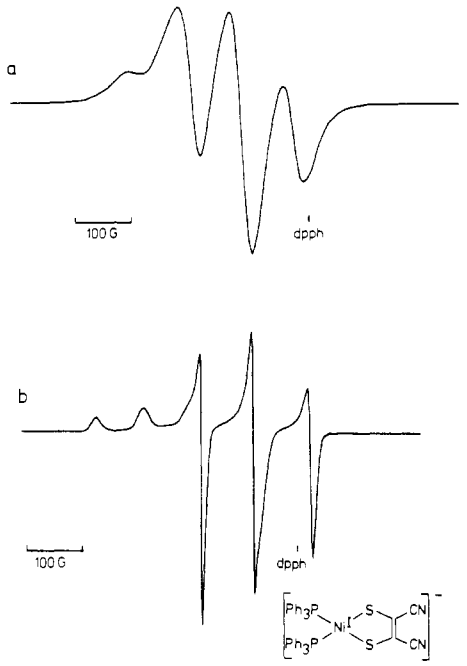

Figure 4. ESR spectra of $[Ni^{I}(PPh_3)((CN)_2C_2S_2)]^-$ electrogenerated CH_2Cl_2 at −40 °C: (a) solution spectrum at −40 °C; (b) frozen-solution spectrum at −160 °C.

inverse of the added triphenylphosphine concentration (Figure 6). This result can be explained if it is assumed that the decay of the Ni^{I} species is preceded by a dissociation equilibrium involving loss of a molecule of PPh_3 from the initially formed complex, i.e.

$$[Ni^{I}(PPh_3)_2((CN)_2C_2S_2)]^- \overset{K}{\rightleftharpoons} [Ni^{I}(PPh_3)((CN)_2C_2S_2)]^- + PPh_3 \quad (6)$$

$$[Ni^{I}(PPh_3)((CN)_2C_2S_2)]^- \xrightarrow{k} \text{ESR-inactive product(s)} \quad (7)$$

If these are rewritten in the general form

$$A \overset{K}{\rightleftharpoons} B + D \quad (8)$$

$$B \xrightarrow{k} C \quad (9)$$

where K is the equilibrium constant for dissociation 6

$$K = [B][D]/[A] \quad (10)$$

and k is the rate constant for the first-order decomposition (7)

$$d[C]/dt = k[B] \quad (11)$$

Substituting (10) into (11)

$$d[C]/dt = (kK/[D])[A] \quad (12)$$

With the assumption that the concentration of B is small compared with that of A and C, i.e., that B is a reactive intermediate

$$d[C]/dt = -d[A]/dt \quad (13)$$

Comparison of (12) and (13) gives

$$-d[A]/dt = (kK/[D])[A] \quad (14)$$

or

$$-d[A]/dt = k'[A] \quad (15)$$

This represents a first-order decay of A with an apparent rate constant

$$k' = kK/[D] = kK/[PPh_3] \quad (16)$$

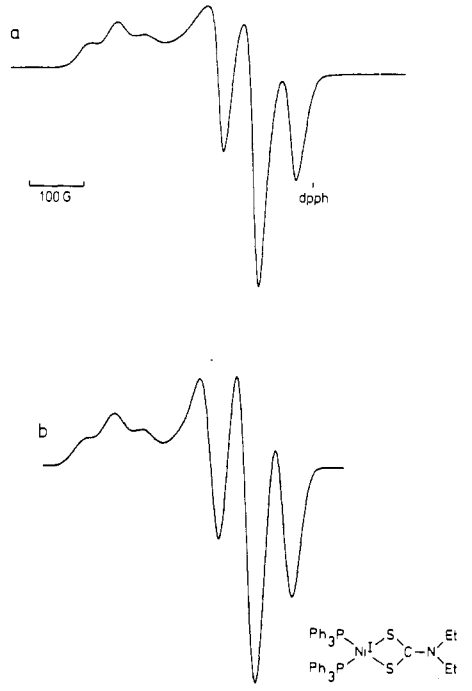

Figure 5. Frozen-solution ESR spectrum of electrogenerated $[Ni^{I}(PPh_3)_2Et_2NCS_2]$ in CH_2Cl_2 at −160 °C: (a) experimental; (b) simulated with $\alpha = 90°$, $g_x = g_y = 2.067$, $g_z = 2.247$, $A_x = 71.2$, $A_y = A_z = 55.2 \times 10^{-4}$ cm^{-1}, $\sigma_x = \sigma_y = 17.0$, and $\sigma_z = 22.0$ G.

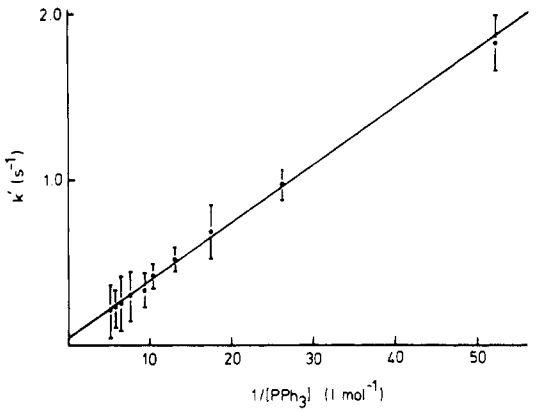

Figure 6. Plot of apparent rate constant k' for the first-order decay of electrogenerated $[Ni^{I}(PPh_3)_2((CN)_2C_2S_2)]^-$ vs. inverse of the added triphenylphosphine concentration.

which is inversely proportional to the concentration of added PPh_3, as observed experimentally.

Like the corresponding dpe complexes, these compounds did not show any reversible oxidation processes.

Reduction and Oxidation of $Ni^{II}(dpe)(C_6H_4O_2)$ and Related Complexes. The cyclic voltammograms of complexes of this type showed both reduction and oxidation processes (Figure 7). The cyclic voltammetry parameters are listed in Table I. The reductions generally showed a larger separation between the anodic and cathodic peaks than those for the corresponding dithiolate complexes, and this peak separation increased with increasing scan rate, indicating a rate-limiting electron-transfer step.

These compounds all yielded ESR spectra when reduced in the in situ ESR cell at the appropriate potential. The solution spectra showed hyperfine coupling to two equivalent ^{31}P nuclei, and the frozen-solution spectra showed anisotropy in the g values and the ^{31}P hyperfine coupling (Figure 8). The ESR parameters obtained from the spectra are listed in Table II.

Electrolysis of these complexes in the in situ ESR cell at the potential of the oxidation peak produced strong ESR

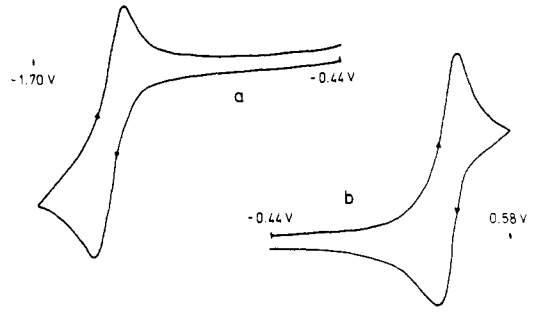

Figure 7. Cyclic voltammogram of $Ni^{II}(dpe)(C_6H_4O_2)$ in CH_2Cl_2 (scan rate = 200 mV s^{-1}): (a) electroreduction of the complex, followed by reoxidation of the reduction product; (b) electrooxidation of the complex, followed by rereduction of the oxidation product.

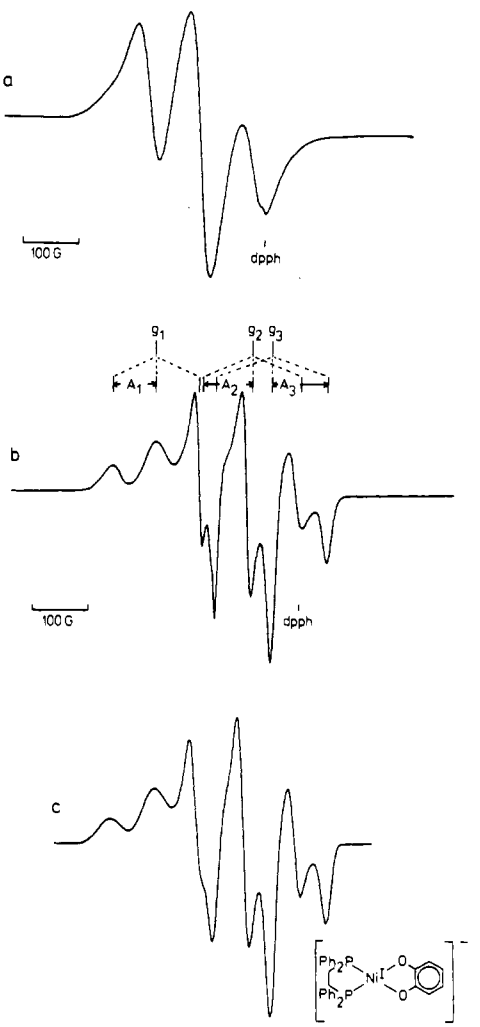

Figure 8. ESR spectra of $[Ni^{I}(dpe)(C_6H_4O_2)]^-$ electrogenerated in CH_2Cl_2 at −60 °C: (a) solution spectrum at −60 °C; (b) frozen-solution spectrum at −160 °C; (c) simulated frozen-solution spectrum with $\alpha = 60.5°$, $g_x = 2.061$, $g_y = 2.032$, $g_z = 2.174$, $A_x = 101.2$, $A_y = A_z = 78.8 \times 10^{-4}$ cm^{-1}, $\sigma_x = \sigma_y = 8.0$, and $\sigma_z = 20.0$ G.

spectra. In the case of the catecholate complex, the spectrum (Figure 9) shows well-resolved hyperfine structure which can be attributed to two sets of two equivalent $I = {}^1/_2$ nuclei. In the case of the tetrachlorocatecholate complex the product was less stable, but its ESR spectrum showed hyperfine structure due to two equivalent $I = {}^1/_2$ nuclei. These results suggest that for the catecholate complex, one of the coupling constants is due to interaction of the unpaired electron with the two equivalent ^{31}P nuclei of the dpe ligand and that the other is due to one of the two sets of equivalent protons of the catecholate ligand. It is surprising that coupling to both sets of

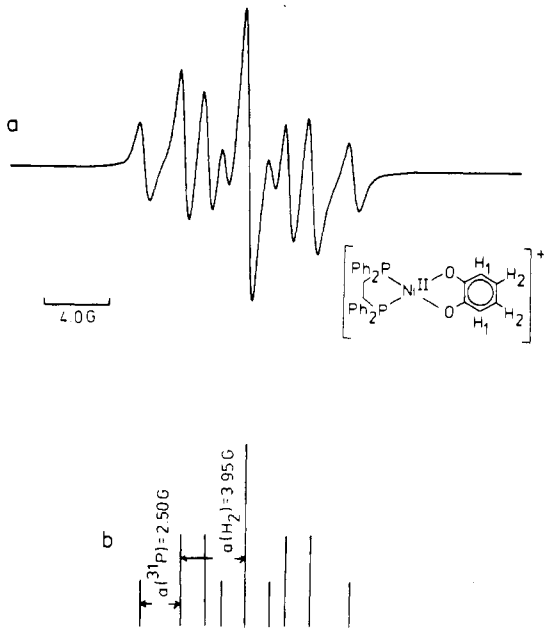

Figure 9. ESR spectrum of $[Ni^{II}(dpe)(C_6H_4O_2)]^+$ electrogenerated in CH_2Cl_2 at −60 °C: (a) experimental; (b) stick-diagram simulation.

Table III. ESR Parameters for Nickel Complexes Produced by One-Electron Oxidation of Ni(dpe)L (L = Catecholate or Substituted Catecholate Ligand)

complex	hyperfine coupling constants, G	g
$[Ni(dpe)(C_6H_4O_2)]^+$	2.50 (2 × ^{31}P), 3.95 ($H_{4,5}$)	2.004
$[Ni(dpe)(CH_3C_6H_3O_2)]^+$	2.34 (2 × ^{31}P), 4.11 (H_4), 0.25 (H_3, H_6), 5.48 (3 × H_{Me})	2.004
$[Ni(dpe)(t\text{-}BuC_6H_3O_2)]^+$	2.34 (2 × ^{31}P), 4.05 (H_5)	2.004
$[Ni(dpe)(C_6Cl_4O_2)]^+$	2.4 (2 × ^{31}P)	2.007

protons is not seen since two coupling constants with ratios ranging from 4 to 8 have been observed for *O*-benzosemiquinone (the one-electron oxidation product of the catecholate ion) and several of its complexes with metal ions. However, it has been shown that the spin density at the carbon atoms in the 3- and 6-positions approaches zero as the interaction of the metal ion with the semiquinone increases.[25] The low value of the spin density at these positions is a consequence of the fact that the unpaired electron orbital in the semiquinone has a nodal plane near these points. Apparently this nodal plane lies almost exactly at these positions in the nickel complex studied here. Thus the couplings are assigned as in Table III with $a_3 = a_6 = 0$. So that this could be confirmed, the 4-methyl- and 4-*tert*-butylcatecholate complexes listed in Table III were also studied. These showed reversible oxidations with parameters as indicated in Table II. The ESR spectra were more complex than that for the symmetrical unsubstituted catecholate compound, but these could be analyzed to yield the parameters listed in Table III. In the case of the 4-methylcatecholate complex all of the proton couplings were resolved, as well as the coupling to the ^{31}P atoms of the dpe ligand. The fact that the magnitude of the ^{31}P coupling is similar in all cases suggests that the assignments made for the unsubstituted catecholate complex are correct.

The proton couplings for these compounds are very similar to those for the free semiquinone ions. This suggests that they are best regarded as Ni^{II} complexes of semiquinone ligands, i.e., that the oxidation essentially involves the catecholate ligand only, as has been previously postulated for oxidation products of catecholate complexes of the type $[Ni^{II}(catecholate)_2]^{2-}$.[13]

(25) Eaton, D. R. *Inorg. Chem.* **1964**, *3*, 1268.

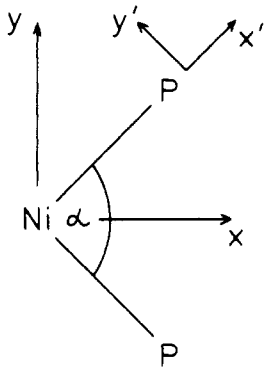

Figure 10. Principal axes of the **g** and phosphorus hyperfine coupling tensors in square-planar Ni^{I} complexes with two cis phosphorus donor atoms (the z and z' axes are perpendicular to the page).

This conclusion is supported by the much lower observed values for the ^{31}P hyperfine coupling constants compared with those for the corresponding one-electron reduction products, where reduction is believed to take place at the metal atom, and the unpaired electron would be expected to interact more strongly with the phosphine ligand. Further support for this idea comes from the observation that the frozen-solution spectra are nearly isotropic, as expected for species which are essentially organic radical ions.

Mixed-ligand Pt and Pd complexes containing PPh_3 and coordinated semiquinone ligands have been reported previously.[14,16] These were obtained by chemical or electrochemical oxidation of the corresponding catecholate complexes and show ^{31}P hyperfine coupling constants similar in magnitude to those observed here for the Ni^{II}(dpe)(catecholate) oxidation products.

Analysis of the Ni^{I} ESR Spectra. The parameters g_1, g_2, g_3, A_1, A_2, and A_3 measured from the frozen-solution ESR spectra of the Ni^{I} complexes were obtained as shown in Figure 8. As discussed previously for the case of the [Ni^{I}(dpe)(R_2NCS_2)] complexes which showed similar spectra, A_2 and A_3 are not the principal components of the ^{31}P hyperfine coupling tensor since the principal axes of the ^{31}P tensor are not expected to coincide with the principal axis of the **g** tensor.[6] The expected relative orientations of the g and hyperfine principal axis systems is shown in Figure 10. It can be shown that for any arbitrary orientation of the magnetic field defined by the unit vector (l_x, l_y, l_z) there will in general be four hyperfine transitions corresponding to the four possible sets of values of the magnetic quantum numbers $M_1 = \pm^1/_2$ and $M_2 = \pm^1/_2$ of the two ^{31}P nuclei. The field positions B for these transitions are given to first order by the resonance condition

$$h\nu = g\beta B + K_1M_1 + K_2M_2 \tag{17}$$

where

$$g^2 = g_x^2l_x^2 + g_y^2l_y^2 + g_z^2l_z^2 \tag{18}$$

$$K_1^2g^2 = A_x^2[l_xg_x\cos(\alpha/2) + l_yg_y\sin(\alpha/2)]^2 + A_{y'}^2[l_xg_x\sin(\alpha/2) - l_yg_y\cos(\alpha/2)]^2 + A_z^2l_z^2g_z^2 \tag{19}$$

$$K_2^2g^2 = A_x^2[l_xg_x\cos(\alpha/2) - l_yg_y\sin(\alpha/2)]^2 + A_{y'}^2[l_xg_x\sin(\alpha/2) + l_yg_y\cos(\alpha/2)]^2 + A_z^2l_z^2g_z^2 \tag{20}$$

and α is the P–Ni–P bond angle (here it is assumed that the principal axis of the phosphorus hyperfine tensor is parallel to the Ni–P bond direction). These expressions were incorporated in the ESR simulation program[6] to allow simulation of the frozen-solution spectra in the presence of the anisotropic phosphorus hyperfine coupling.

In order to carry out the simulations it is necessary to obtain an estimate of the values of the principal components of the phosphorus hyperfine coupling tensor and of the angle α. The coupling constant A_1 measured from the "parallel" region of the spectrum (Figure 8) corresponds to the principal z axis of the **g** tensor and the z' axis of the phosphorus hyperfine tensor. Thus $A_1 = A_z = A_{z'}$. The coupling constants A_2 and A_3 measured from the "perpendicular" region correspond to the effective splittings A_x and A_y along the x and y axis of the **g** tensor (although not necessarily in that order) and are related to the principal components $A_{x'}$ and $A_{y'}$ by eq[6] 21 and 22.

$$A_x^2 = A_{x'}^2\cos^2(\alpha/2) + A_{y'}^2\sin^2(\alpha/2) \tag{21}$$

$$A_y^2 = A_{x'}^2\sin^2(\alpha/2) + A_{y'}^2\cos^2(\alpha/2) \tag{22}$$

When $\alpha = 90°$, eq 23 obtains. This is apparently the case for

$$A_x^2 = A_y^2 = {}^1/_2(A_{x'}^2 + A_{y'}^2) \tag{23}$$

the PPh_3 complexes listed in Table II which show essentially axially symmetric spectra ($A_2 = A_3$). If it is assumed that the phosphorus hyperfine tensor is axially symmetric about the Ni–P bond direction (the x' direction), then $A_{y'} = A_{z'} = A_1$. $A_{x'}$ can then be obtained from eq 21 and 22 which yield eq 24. A simulation of the spectrum of [$Ni^{I}(PPh_3)_2(Et_2NCS_2)$] with hyperfine coupling parameters obtained in this manner gives good agreement with the experimental spectrum (Figure 5). This simulation is not unique so care is necessary in interpreting the hyperfine coupling parameters obtained. However, it is worth noting that the values obtained are exactly those expected for transfer of 0.07 of an unpaired electron to a phosphorus sp^3-hybrid orbital which lies along the Ni–P bond direction. This can be shown as follows. The observed anisotropic ^{31}P coupling constants $A_{x'}$, $A_{y'}$, and $A_{z'}$ consist of an isotropic term a and anisotropic dipolar coupling terms $A_{x'}'$, $A_{y'}'$, and $A_{z'}'$ due to direct magnetic dipole–dipole coupling between the unpaired electron and the ^{31}P nucleus

$$A_{x'} = a + A_{x'}' \qquad A_{y'} = a + A_{y'}' \qquad A_{z'} = a + A_{z'}' \tag{25}$$

$$A_{x'}^2 + A_y^2 = A_{x'}^2 + A_{y'}^2 \tag{24}$$

The isotropic term a, which results from a Fermi contact interaction, is generally much larger than the other terms so the sign of a (which in this case is expected to be positive) determines the sign of $A_{x'}$, $A_{y'}$, and $A_{z'}$. Since

$$A_{x'}' + A_{y'}' + A_{z'}' = 0 \tag{26}$$

the isotropic term can be obtained from

$$a = {}^1/_3(A_{x'} + A_{y'} + A_{z'})$$

and the dipolar terms can be obtained from (25). This yields (27). The ^{31}P hyperfine coupling parameters for the phosphorus 3s and 3p orbitals are $A = 3436 \times 10^{-4}$ cm^{-1} and $B = 189 \times 10^{-4}$ cm^{-1}, respectively.[26] For a single unpaired electron in an sp^3-hybrid orbital along the x' direction, the parameters corresponding to (27) would be

$$a = {}^1/_4A = 859 \times 10^{-4}\ \text{cm}^{-1}$$
$$A_{x'}' = {}^3/_4B = 142 \times 10^{-4}\ \text{cm}^{-1} \tag{28}$$
$$A_{y'}' = A_{z'}' = {}^3/_4(B/2) = 71 \times 10^{-4}\ \text{cm}^{-1}$$

The ratio of the corresponding quantities in (27) and (28) is 0.07, and this corresponds to the amount of spin density in the

$$a = 60.5 \times 10^{-4}\ \text{cm}^{-1} \qquad A_{x'}' = 10.7 \times 10^{-4}\ \text{cm}^{-1}$$
$$A_{y'}' = A_{z'}' = -5.3 \times 10^{-4}\ \text{cm}^{-1} \tag{27}$$

(26) Goodman, B. A.; Raynor, J. B. *Adv. Inorg. Chem. Radiochem.* **1970**, *13*, 135.

phosphorus sp^3 orbital. This represents the spin density transferred from the Ni 3d orbital to the phosphorus sp^3 donor orbital as a result of partial Ni–P covalent bonding. It can be noted that there appears to be no evidence of spin polarization effects of the type postulated by Labauze and Raynor to account for the values of the ^{31}P hyperfine coupling constants in some cobalt(II) complexes of PPh_3 and related ligands.[27]

The nickel(I) bis(diphenylphosphino)ethane complexes show some degree of axial asymmetry in the observed hyperfine coupling parameters ($A_2 \neq A_3$). This implies $A_x \neq A_y$, and this can only occur if α is not equal to 90° (eq 23). (A P–M–P bond angle in the range 75–90° is expected on the basis of crystal structure studies on other transition-metal dpe complexes.[28]) Again, $A_{z'} = A_z = A_1$, and if the phosphorus hyperfine tensor is taken to be axially symmetric, with $A_{y'} = A_{z'}$, eq 24 can be used to determine $A_{x'}$. The analysis of the $[Ni^I(dpe)(C_6H_4O_2)]^-$ spectrum is given below as a typical example. The hyperfine coupling parameters obtained in the above way correspond to $\alpha = 60°$ (from eq 21 and 22 with $A_x = A_3$ and A_y and A_2), but reasonable simulations of the observed spectrum can be obtained for α in the range 50–70°. The simulation for $\alpha = 60°$ is shown in Figure 8. It is not necessary that the phosphorus hyperfine tensor have axial symmetry, of course, and reasonable simulations of the observed spectrum can be obtained for other angles α and appropriate phosphorus hyperfine coupling constants. However, the maximum angle α in the range 0–90° for which a reasonable fit can be obtained is about 70°. For angles closer to 90° and approximately axially symmetric hyperfine coupling, the difference between A_2 and A_3 is not as large as in the observed spectrum, while for a large degree of axial asymmetry the central doublet in the perpendicular region of the spectrum shows a considerably larger splitting than that observed experimentally. This apparently occurs because the turning points in the field position as a function of angle of orientation of the applied field do not occur along the principal axis of the **g** tensor. They occur instead at an intermediate orientation where the coupling constants K_1 and K_2 for the two phosphorus atoms are not equal.

The above analysis is based on the assignments $g_x = g_3$, $g_y = g_2$, $A_x = A_3$, and $A_y = A_2$ which correspond to values of α in the range 0–90°. The opposite assignments, $g_x = g_2$, $g_y = g_3$, $A_x = A_3$, and $A_y = A_2$, correspond to values of α in the range 90–180°. In fact the computed spectrum for any value of α in the range 0–90° for the first assignment is identical with the spectrum obtained for 180° − α for the second assignment. Thus the simulated spectrum in Figure 8 for $\alpha = 60°$ also corresponds to $\alpha = 120°$. However, the minimum angle in the range 90–180° for which a reasonable simulation can be obtained is 110°. This seems too large for the bond angle concerned.

Thus it appears that the observed inequality of the two phosphorus hyperfine coupling parameters in the perpendicular region of the spectrum cannot be readily understood in terms of the expected values of $A_{x'}$, $A_{y'}$, and α. One possible explanation of this is that the principal axes x' for the two phosphorus atoms do not lie along the Ni–P bonds but lie in such a direction that they intersect at an angle of say 60–70°. Again, since the simulation is not unique, care is necessary in interpreting the hyperfine coupling parameters obtained. However, one notable features of the results is that the ^{31}P hyperfine coupling parameters $A_{x'}$, $A_{y'}$, and $A_{z'}$ for this complex are 1.4 times as large as those for $Ni^I(PPh_3)_2(Et_2NCS_2)$, which were shown above to indicate a spin density of 0.07 in the phosphorus donor orbital. A similar treatment for the dpe complex therefore yields a spin density of 1.4 × 0.07 = 0.10 in the phosphorus donor orbital of dpe. Similar results were obtained for the other dpe complexes, all of which show higher ^{31}P hyperfine coupling constants than the PPh_3 complexes. This suggests that dpe is a better σ donor than PPh_3 since the higher the degree of charge transfer from the phosphine to the metal orbital, the higher the corresponding transfer of spin density from the metal orbital to the phosphine.

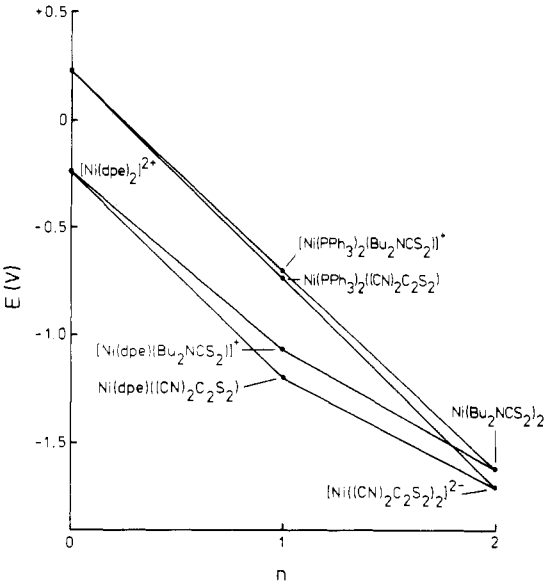

Figure 11. Reduction potentials as a function of n for the series of compounds $[Ni(dpe)_{2-n}(R_2NCS_2)_n]^{(2-n)+}$, $[Ni(dpe)_{2-n}((CN)_2C_2S_2)_n]^{(2-2n)+}$, $[Ni(PPh_3)_{4-2n}(R_2NCS_2)_n]^{(2-n)+}$, and $[Ni(PPh_3)_{4-2n}((CN)_2C_2S_2)_n]^{(2-2n)+}$.

We have previously shown from an analysis of the g values and ^{61}Ni hyperfine coupling constants for $[Ni^I(Bu_2NCS_2)_2]^-$ that unpaired spin density corresponding to 0.2e is transferred from the Ni atom to the dithiocarbamate ligands.[6] This corresponds to a transferred spin density of 0.1 to each dithiocarbamate ligand. This, combined with the above ^{31}P hyperfine coupling results, shows that delocalization of spin density onto the ligand increases along the series $R_2NCS_2^- < 2PPh_3 <$ dpe. This is consistent with the observation that the g values decrease along the series of compounds $[Ni^I(R_2NCS_2)_2]^- > Ni^I(PPh_3)_2(R_2NCS_2) > Ni^I(dpe)(R_2NCS_2) > [Ni^I(dpe)_2]^+$ since the g values are expected to approach 2 as the extent of delocalization of the unpaired electron from the metal atom increases. Thus the above analysis of the ESR parameters seems to provide consistent description of the bonding in the nickel(I) complexes studied.

The Reduction Potentials. Several authors have shown that the oxidation potentials of mixed-ligand complexes such as $[M(CO)_{6-n}L_n]^{y+}$ (M = Cr, Mn) change in a regular manner when CO is replaced by L, a linear relationship between $E_{1/2}$ and n being observed in several cases. This is believed to be a consequence of the fact that the ligand influence on the energy of the HOMO is additive for isostructural complexes, and this has been used as a basis for the definition of a ligand constant, P_L, which is a direct measure of the effect on the oxidation potential of replacement of the reference ligand CO by L. The P_L values are believed to reflect the combined σ-donor plus π-acceptor properties of L.[29] The additive influence of ligands on the HOMO energy has been demonstrated by molecular orbital calculations.[30] A similar situation is expected to exist for reduction potentials since these depend

(27) Labauze, G. L.; Raynor, J. B. *J. Chem. Soc., Dalton Trans.* **1981**, 590.
(28) Rehder, D.; Müller, I.; Kopf, J. *J. Inorg. Nucl. Chem.* **1978**, *40*, 1013.
(29) Chatt, J.; Kan, C. T.; Leigh, G. J.; Pickett, C. J.; Stanley, D. R. *J. Chem. Soc., Dalton Trans.* **1980**, 2032.
(30) Sarapu, A. C.; Fenske, R. F. *Inorg. Chem.* **1975**, *14*, 247.

on the LUMO energy which should be affected by ligand substitution in the same way.

We find that a similar additivity principle is approximately obeyed by the two series of complexes $[Ni(dpe)_{2-n}(S_2CNR_2)_n]^{(2-n)+}$ and $[Ni(dpe)_{2-n}((CN)_2C_2S_2)_n]^{(2-2n)+}$ (n = 0-2). The reduction potentials for these compounds as a function of n are given in Figure 11. It is clear from this diagram that the reduction potential varies in an approximately linear manner with n, where results for the n = 0-2 complexes are available (the dpe series). The results for the n = 1 compounds show that replacement of one dithiolate ligand in the bis(dithiolate) complexes by two molecules of PPh_3 cause the reduction to shift to considerably more positive potentials than does the corresponding replacement by bis(diphenylphosphino)ethane.

So that the additivity principle for the $[Ni(PPh_3)_{2(2-n)}(R_2NCS_2)_n]^{(2-n)+}$ and $[Ni(PPh_3)_{2(2-n)}((CN)_2C_2S_2)_n]^{(2-2n)+}$ complexes could be tested, the potential for the one-electron reduction of $[Ni^{II}(PPh_3)_4]^{2+}$ is required. Extrapolation of the lines through the n = 1 and 2 points to n = 0 suggests that this should occur at a potential of +0.2 V (Figure 11). The reduction of Ni^{2+} in the presence of excess PPh_3 in acetonitrile has been studied by other workers, but the reduction appears to involve the species $[Ni^{II}(PPh_3)_2(CH_3CN)_4]^{2+}$ and is a two-electron process which results in the formation of the zerovalent complex $Ni(PPh_3)_4$. This then reacts with the Ni^{II} complex present to produce $[Ni^{I}(PPh_3)_4]^{+}$, which can be irreversibly oxidized at a potential of about +0.4 V relative to SCE.[31] In an attempt to observe the reversible one-electron reduction of $[Ni^{II}(PPh_3)_4]^{2+}$, we carried out similar experiments in CH_2Cl_2, which has a lower coordinating ability than CH_3CN. However, even in the presence of a very large excess of PPh_3, the redox behavior was found to be similar to that in CH_3CN. The cathodic peak due to the irreversible oxidation of $[Ni^{I}(PPh_3)_4]^{+}$ occurs at +0.23 V, near to the value predicted in Figure 11 for the reversible process.

The greater ease of reduction (i.e., the less negative reduction potential) of the bis(triphenylphosphine) complexes compared with the dpe complexes may be related to the relative strength of the metal-phosphorus interactions. The reduction potential is determined, in part, by the energy of the LUMO which the electron occupies after electron transfer. If the LUMO is high in energy, a greater free energy change occurs on reduction at a more negative reduction potential.[32] The ESR parameters for the Ni^{I} complexes produced on reduction of the corresponding Ni^{II} complexes suggest that the degree of σ-covalent bonding is greater in the dpe than PPh_3 compounds. If this is also true, the LUMO occupied by the unpaired electron on reduction is *higher* in energy for the dpe complexes, leading to a *more negative* reduction potential than the corresponding PPh_3 complexes. While this explanation appears to describe well these results, a great many other factors may also affect the reduction potentials (such as metal phosphorus π interactions and differing solvation energies of oxidized and reduced species). A more complete discussion should take into consideration the change in total electronic energy of the complex as it goes from Ni^{II} to Ni^{I} rather than considering the energy of a single orbital in the parent Ni^{II} complex. However, in the spirit of the frozen-orbital approximation, it is possible to relate total energy changes to changes in single-orbital occupancy.

Acknowledgment. We wish to thank the New Zealand University Grants Committee and the New Zealand Energy Research and Development Committee for financial assistance. We also wish to thank Dr. G. A. Wright for the use of electrochemical equipment.

Registry No. $Ni(dpm)((CN)_2C_2S_2)$, 81097-94-1; $Ni(dae)((CN)_2C_2S_2)$, 81097-95-2; $Ni(dpe)((CN)_2C_2S_2)$, 81097-96-3; $Ni(dpe)(O_2C_2S_2)$, 81097-97-4; $Ni(dpe)(CS_3)$, 81097-98-5; $Ni(dpe)(CH_3C_6H_3S_2)$, 81097-99-6; $Ni(dpe)(C_6H_4(CH_2S)_2)$, 81098-00-2; $Ni(dpe)(C_6H_4O_2)$, 79948-89-3; $Ni(dpe)(CH_3C_6H_3O_2)$, 81098-01-3; $Ni(dpe)(t\text{-}BuC_6H_3O_2)$, 81098-02-4; $Ni(dpe)(C_6Cl_4O_2)$, 38107-43-6; $Ni(dpb)((CN)_2C_2S_2)$, 81098-03-5; $Ni(PPh_3)_2((CN)_2C_2S_2)$, 81098-04-6; $[Ni(PPh_3)_2(Et_2NCS_2)]^{+}$, 55060-26-9; $[Ni(PPh_3)_2(Bu_2NCS_2)]^{+}$, 55060-27-0; $[Ni(PPh_3)_2(Bzl_2NCS_2)]^{+}$, 81098-05-7; $[Ni(PPh_3)_2(Cy_2NCS_2)]^{+}$, 81098-06-8; $[Ni((CN)_2C_2S_2)_2]^{2-}$, 14876-79-0; $Ni(PPh_3)_2(Et_2NCS_2)$, 81141-90-4; $Ni(PPh_3)_2(Bu_2NCS_2)$, 81195-35-9; $Ni(PPh_3)_2(Bzl_2NCS_2)$, 81157-73-5; $Ni(PPh_3)_2(Cy_2NCS_2)$, 81098-07-6; $[Ni(PPh_3)_2((CN)_2C_2S_2)]^{-}$, 81098-08-0; $[Ni(dpe)((CN)_2C_2S_2)]^{-}$, 81098-09-1; $[Ni(dpm)((CN)_2C_2S_2)]^{-}$, 81098-10-4; $[Ni(dpb)((CN)_2C_2S_2)]^{-}$, 81098-11-5; $[Ni(dae)((CN)_2C_2S_2)]^{-}$, 81098-12-6; $[Ni(dpe)(CH_3C_6H_3S_2)]^{-}$, 81098-13-7; $[Ni(dpe)(O_2C_2S_2)]^{-}$, 81098-14-8; $[Ni(dpe)(CS_3)]^{-}$, 81098-15-9; $[Ni(dpe)(C_6Cl_4O_2)]^{-}$, 81098-16-0; $[Ni(dpe)(C_6H_4O_2)]^{-}$, 81098-17-1; $[Ni(dpe)(C_6H_4O_2)]^{+}$, 81098-18-2; $[Ni(dpe)(CH_3C_6H_3O_2)]^{+}$, 81098-19-3; $[Ni(dpe)(t\text{-}BuC_6H_3O_2)]^{+}$, 81098-20-6; $[Ni(dpe)(C_6Cl_4O_2)]^{+}$, 81098-21-7; $Ni(dpe)Cl_2$, 14647-23-5.

(31) Bontempelli, G.; Magno, F.; Corain, B.; Schiavon, G. *J. Electroanal. Chem. Interfacial Electrochem.* **1979**, *103*, 243.

(32) Bard, A. J.; Faulkner, L. R. "Electrochemical Methods"; Wiley: New York, 1980; Chapter 1.

Contribution from the Department of Chemistry, University of California, Davis, California 95616

Preparation and Characterization of Some Hydroxy Complexes of Iron(III) Porphyrins

RU-JEN CHENG, LECHOSLAW LATOS-GRAZYNSKI, and ALAN L. BALCH*

Received December 1, 1981

Oxidation of $(TMP)Fe^{II}$ or $(T(2,4,6\text{-}MeO)_3PP)Fe^{II}$ (TMP is the dianion of *meso*-tetramesitylporphyrin; $T(2,4,6\text{-}MeO)_3PP$ is the dianion of *meso*-tetrakis(2,4,6-trimethoxyphenyl)porphyrin) yields (TMP)FeOH or $(T(2,4,6\text{-}MeO)_3PP)FeOH$. These same hydroxy complexes are obtained by treating the corresponding $PFe^{III}Cl$ (P is a generalized porphyrin dianion) with aqueous sodium hydroxide. Complexes of the type PFeOH are distinguished from the more common oxo-bridged dimers PFeOFeP on the basis of ^1H NMR spectra, magnetic susceptibilities, infrared spectroscopy, and electron spin resonance spectroscopy. These hydroxy complexes behave as typical high-spin, five-coordinate iron(III) compounds. Mixtures of PFeOH and PFeOFeP are formed when P is *meso*-tetrakis(3,4,5-trimethoxyphenyl)porphyrin dianion or *meso*-tetrakis(perfluorophenyl)porphyrin dianion.

Introduction

Iron(III) porphyrin compounds of the type PFeX are high-spin ($S = {}^5/_2$), five-coordinate complexes. In the late 1960s it was realized that complexes previously formulated as the hydroxy compounds PFeOH, and believed then to be members of the class of PFeX compounds, were actually

0020-1669/82/1321-2412$01.25/0